How to cite: *Angew. Chem. Int. Ed.* **2024**, *63*, e202403636
doi.org/10.1002/anie.202403636

VIP Medicinal Chemistry Very Important Paper

Photoswitchable Carbamazepine Analogs for Non-Invasive Neuroinhibition *In Vivo*

*Luisa Camerin, Galyna Maleeva[+], Alexandre M. J. Gomila[+], Irene Suárez-Pereira, Carlo Matera, Davia Prischich, Ekin Opar, Fabio Riefolo, Esther Berrocoso, and Pau Gorostiza**

Abstract: A problem of systemic pharmacotherapy is off-target activity, which causes adverse effects. Outstanding examples include neuroinhibitory medications like antiseizure drugs, which are used against epilepsy and neuropathic pain but cause systemic side effects. There is a need of drugs that inhibit nerve signals locally and on-demand without affecting other regions of the body. Photopharmacology aims to address this problem with light-activated drugs and localized illumination in the target organ. Here, we have developed photoswitchable derivatives of the widely prescribed antiseizure drug carbamazepine. For that purpose, we expanded our method of *ortho* azologization of tricyclic drugs to *meta*/*para* and to N-bridged diazocine. Our results validate the concept of *ortho* cryptoazologs (uniquely exemplified by Carbazopine-**1**) and bring to light Carbadiazocine (**8**), which can be photoswitched between 400–590 nm light (using violet LEDs and halogen lamps) and shows good drug-likeness and predicted safety. Both compounds display photoswitchable activity *in vitro* and in translucent zebrafish larvae. Carbadiazocine (**8**) also offers *in vivo* analgesic efficacy (mechanical and thermal stimuli) in a rat model of neuropathic pain and a simple and compelling treatment demonstration with non-invasive illumination.

Introduction

Pharmacotherapy is the treatment of choice for many diseases. Using small molecule drugs to target pathophysiological processes has several advantages: fast, simple, and often non-invasive delivery, well-defined mechanism of action, dosage control, and predictable pharmacokinetics. However, a persistent problem with systemically administered drugs is their off-target activity and resulting adverse effects. Even highly selective drugs that bind only to a particular receptor type can produce side effects if it is expressed in multiple tissues or organs, as it is generally difficult to control the drug distribution within the body and prevent its interaction with the same receptor expressed in other regions than the target organ. A paradigmatic example is chemotherapy,[1] in which the intended activity of the

[*] L. Camerin, G. Maleeva,[+] A. M. J. Gomila,[+] C. Matera, D. Prischich, E. Opar, F. Riefolo, P. Gorostiza
Institute for Bioengineering of Catalonia (IBEC), The Barcelona Institute for Science and Technology, Barcelona, 08028 Spain
E-mail: pau@icrea.cat

L. Camerin, G. Maleeva,[+] A. M. J. Gomila,[+] C. Matera, D. Prischich, E. Opar, F. Riefolo, P. Gorostiza
Networking Biomedical Center in Bioengineering, Biomaterials, and Nanomedicine (CIBER-BBN), ISCIII, Madrid, 28029 Spain

L. Camerin
Doctorate program in organic chemistry, University of Barcelona, Barcelona, 08028 Spain

I. Suárez-Pereira, E. Berrocoso
Neuropsychopharmacology & Psychobiology Research Group, Department of Neuroscience, University of Cádiz, Cádiz, 11003 Spain

I. Suárez-Pereira, E. Berrocoso
Networking Biomedical Center in Mental Health (CIBER-SAM), ISCIII, Madrid, 28029 Spain

I. Suárez-Pereira, E. Berrocoso
Institute for Research and Innovation in Biomedical Sciences of Cádiz, INiBICA, University Hospital Puerta del Mar, Cádiz, 11009 Spain

C. Matera
Department of Pharmaceutical Sciences, University of Milan, Milan, 20133 Italy

P. Gorostiza
Catalan Institution of Research and Advanced Studies (ICREA), Barcelona, 08010 Spain

D. Prischich
Current address: Department of Chemistry, Molecular Sciences Research Hub, Imperial College London, London SW120BZ United Kingdom

F. Riefolo
Current address: Teamit Institute, Partnerships, Barcelona Health Hub, Barcelona 08025 Spain

[+] Equivalent contribution.

drugs is indeed cytotoxicity, but the treatments of neurological diseases are particularly representative.[2]

The shortcomings of pharmacotherapy become particularly apparent in the treatment of neuropathic pain, which originates locally at injured nerves and specific brain regions but is treated systemically to reach pharmacological targets in the central nervous system. While inflammatory pain is due to the inflammatory response associated with tissue damage, which increases sensitivity, neuropathic pain is caused by somatosensory system injuries or diseases such as lumbar radiculopathy ("sciatica"), diabetic neuropathy, and chronic postsurgical pain.[3,4] Currently, the management of inflammatory pain with analgesic drugs (non-steroidal anti-inflammatory drugs, NSAIDs) is well-tolerated by patients, but they are not effective in neuropathic pain. Neuro-inhibitory drugs (including antidepressant pain-relievers and antiepileptic drugs, AEDs) have partial efficacy on neuropathic pain but cause systemic adverse effects. Both aspects can be improved by locally injecting lower drug concentrations in the spinal cord with implanted intrathecal pumps,[5] but they are invasive, subject to infections, and require drug refills. An alternative is localized spinal cord stimulation with implanted electrodes and battery-operated electronic stimulators, but it is based on complex devices that may malfunction and require replacement surgery.

Pharmacological treatment of neuropathic pain often necessitates more potent analgesics than NSAIDs (e.g. acetaminophen, ibuprofen), such as opioids. Nevertheless, their usage remains highly contentious due to several factors. Firstly, neuropathic pain does not consistently respond favorably to opioids, and achieving relief often demands high doses, escalating concerns about tolerance and addiction. Additionally, the systemic side effects associated with opioid use, including constipation, nausea, dizziness, and drowsiness, further compound these apprehensions. Drug treatments should also not produce anesthetic or sedative effects that can lead to loss of consciousness (like the general anesthetic propofol or even fomocaine, which must be administered topically). High-quality, evidence-based treatment guidelines advocate for the use of anticonvulsants (AEDs) in managing neuropathic pain. These include medications that target voltage-gated calcium channels (Ca_V, e.g. gabapentin, pregabalin) and blockers of voltage-gated sodium channels (Na_V, e.g., carbamazepine, oxcarbazepine, phenytoin, lamotrigine). However, their doses are still limited by systemic adverse effects, which in turn hamper efficacy and require clinical monitoring.[6] Thus, there is an unmet need for AEDs that inhibit nerve signals on demand and that do not affect other regions or organs susceptible to producing side effects.

To achieve this aim, photopharmacological compounds allow for delivering pharmacological action under the control of light, which can be focused on a target region and can be reversibly switched on and off.[7,8] These compounds comprise bioligand and photoisomerizable moieties, the latter changing the pharmacological properties of the former in an isomer-dependent manner. Thus, photoisomerization with different illumination wavelengths reversibly changes the drug activity and enables light-driven control of its biological target,[7,9] including ion channels,[10] ionotropic receptors,[11–18] G protein-coupled receptors,[19–24] and enzymes[25–28] . Azobenzenes and ultraviolet (UV)-green wavelengths are commonly used in photopharmacology, although red-shifted wavelengths are desirable for deeper tissue penetration and safety.[29–31]

Here, we devised drug-like photoswitchable derivatives of the widely prescribed AED carbamazepine to produce spinal-mediated analgesia on demand in an animal model of neuropathic pain. The rationale behind administering anticonvulsants locally in the spinal cord of the rat is to attenuate nociceptive signals stemming from peripheral nerves while circumventing the systemic side effects associated with general administration. This targeted approach is motivated by the pivotal role of the spinal cord in processing and transmitting nociceptive information to the brain. Notably, we used non-invasive illumination to achieve this effect and did not observe apparent anesthetic, sedative actions, or toxicity.

Carbamazepine was developed to treat epileptic seizures[32] and is useful in managing neuropathic pain, including trigeminal neuralgia, and psychiatric diseases like bipolar disorder.[33,34] It is a small molecule that can permeate the blood–brain barrier and is orally bioavailable. Like other AEDs and local anesthetics (which are even smaller and protonated), it interacts with sodium channels near their pore, but it displays different mechanisms of action (conductance, gating) and therapeutic effects. Reported adverse effects of systemically administered carbamazepine include nausea, vomiting, dizziness, somnolence, diplopia, vertigo, and ataxia. Interestingly, its tricyclic structure is not planar but butterfly-shaped and is amenable to designing photoswitchable azobenzene analogs. For that purpose, we expanded our method of azologization of tricyclic drugs[22] to (1) *meta*/*para* cryptoazologs (including different *ortho* and push-pull substituents, all of which turned out to be inactive, thus validating the original concept demonstrated with *ortho* cryptoazologs) and to (2) diazocine cryptoazologs. The latter revealed effective photoswitching between visible wavelengths 400 nm and 590 nm (which allows using conventional wide-spectrum halogen lamps), good drug-likeness and predicted safety, *in vivo* analgesic activity against neuropathic pain (mechanical and thermal pain), and *in vivo* photoswitching of neuropathic pain analgesia with non-invasive halogen light.

Results and Discussion

Design and Synthesis of Photoswitchable Carbamazepine Analogs

The design of photoswitchable analog of carbamazepine followed a non-trivial azologization approach (dubbed crypto-azologization since the analogy is hidden in the ring structure) that proved to be effective in tricyclic drugs.[22] Here, we expanded this method to include linearized azobenzenes beyond the originally reported *ortho* substitu-

tion (*meta* and *para*) as well as tricyclic diazocines (compounds **1**–**7** and **8**, respectively, Figure 1).

We first examined the structure–activity relationship (SAR) of carbamazepine to identify the position of the pharmacophore and its interaction in the pore of voltage gated sodium channels (Na_V). Carbamazepine is part of a family of anticonvulsant drugs with very conserved structural elements that embrace one aryl ring (R), an electron donor atom (D), and a hydrogen bond acceptor/donor group (HAD), mutually separated by fixed distances.[35,36] In particular, the urea moiety in carbamazepine is involved in an amino-aromatic hydrogen bond in the binding pocket and establishes a crucial interaction for drug recognition.[37]

Therefore, we retained these elements and designed the first cryptoazologs of carbamazepine by opening the seven-membered central ring and replacing it with the azo (–N=N–) bond. We named these linearized analogs "carbazopines". The urea moiety was kept in *ortho* position as in the parent drug[22] but, here, we also explored *meta* and *para* positions to test how flexible are the constraints of the pharmacophore (Figure 1B, Carbazopine-**1**, –**2**, and –**3**, respectively). These structures allow us to probe whether the conformational change upon isomerization localizes the urea functional group in the right cavity and how it depends on the urea substitution position.

Subsequently, we expanded the chemical library by introducing *para* and *ortho* substitutions in the unsubstituted aromatic ring, aiming to tune the photochromic properties (Figure 1C, Carbazopine-**4** to –**7**). In particular, it has been reported that push-pull systems[30] and tetra-*ortho* substitutions with fluorine, chlorine, and methoxy groups[38] produce a red-shift in the absorption spectra of the azo compound that allows *trans* to *cis* conversion at wavelengths toward the red region of the spectrum, which are convenient because they display deeper tissue penetration than UV or blue light. Since the urea occupies the *ortho* position in one of the aromatic rings, we focused on bi-substitutions at the opposite ring.

Furthermore, we designed a photoswitchable analog of carbamazepine, keeping the middle ring closed. Bridged azobenzenes are receiving increasing attention in materials and biology.[8,39,40] We based our approach on *N*-bridged diazocine, which adds an extra carbon atom to the central ring of carbamazepine, and we kept the urea at an equivalent position to that of the drug (Figure 1D, compound **8**). We named it Carbadiazocine (**8**) in subsequent experiments.

Before synthesizing the compounds of Figure 1, we examined their drug-likeness and the predicted safety properties of Carbazopine-**1** and Carbadiazocine (**8**) using ChemDraw and ProTox-II, see Supporting Information (SI). The results are shown in Table S1, S2 and Figures S1, S2, and S3, and predict that all compounds designed by cryptoazologization will retain or improve the drug-likeness and safety of carbamazepine.

Linear azobenzene derivatives Carbazopine-**1** to –**3** were prepared from the respective commercially available *ortho/meta/para* phenylenediamines (Scheme 1A). The urea moiety was introduced with a substitution reaction using as a reagent potassium isocyanate under acidic conditions. The obtained intermediates were subsequently coupled with nitrosobenzene under Mills conditions.

The library of *para* and *ortho* substituted derivatives (Carbazopine-**4** to –**7**) was obtained via a divergent synthetic approach starting from the common intermediate (**9**, Scheme 1B). This intermediate was combined under Mills conditions with commercially available 1,3-dichloro-2-nitrosobenzene and the previously synthesized compound **12**

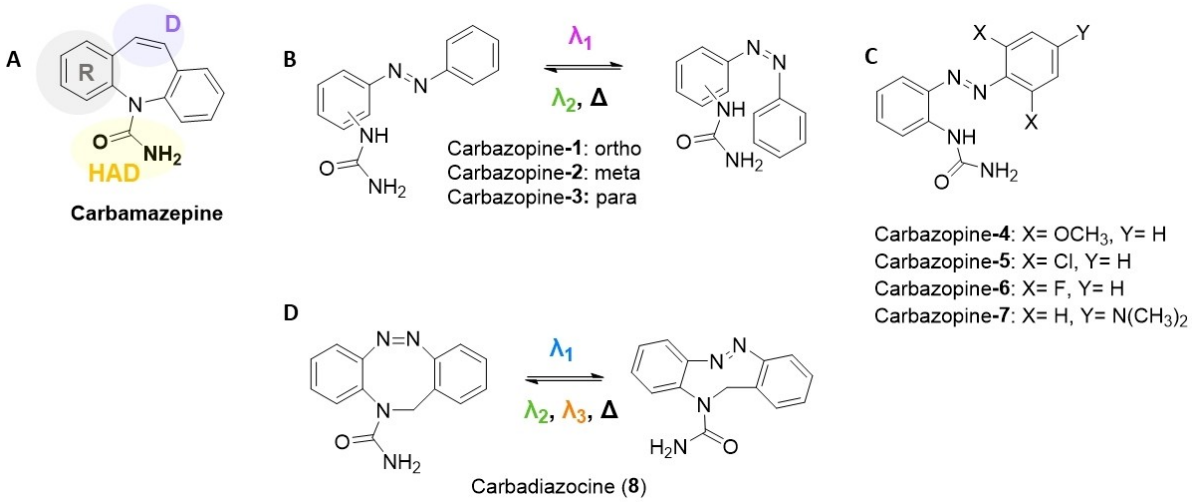

Figure 1. Design of photoswitchable analogs of carbamazepine. **A)** Structure of the neuroinhibitory drug carbamazepine. The structural elements of the pharmacophore are marked as follows: HAD, hydrogen acceptor/donor unit; D, electron donor unit; R, hydrophobic aryl unit.[35,36] **B)** Linearized, ring-opened azobenzene analog[22] of carbamazepine with *ortho*/*meta*/*para* substitution in the left ring. They were named Carbazopine-**1**, –**2**, and –**3**, respectively. Their dark-relaxed *trans* isoform (left) is photoconverted to the *cis* isoform (right). **C)** Substitutions on the right ring of the ortho variant of B (Carbazopine-**1**) were named Carbazopine-**4** to –**7**. **D)** Bridged azobenzene (diazocine) analog of carbamazepine, named Carbadiazocine (**8**). The dark-relaxed *cis* isoform (left) is photoconverted to the *trans* isoform (right).

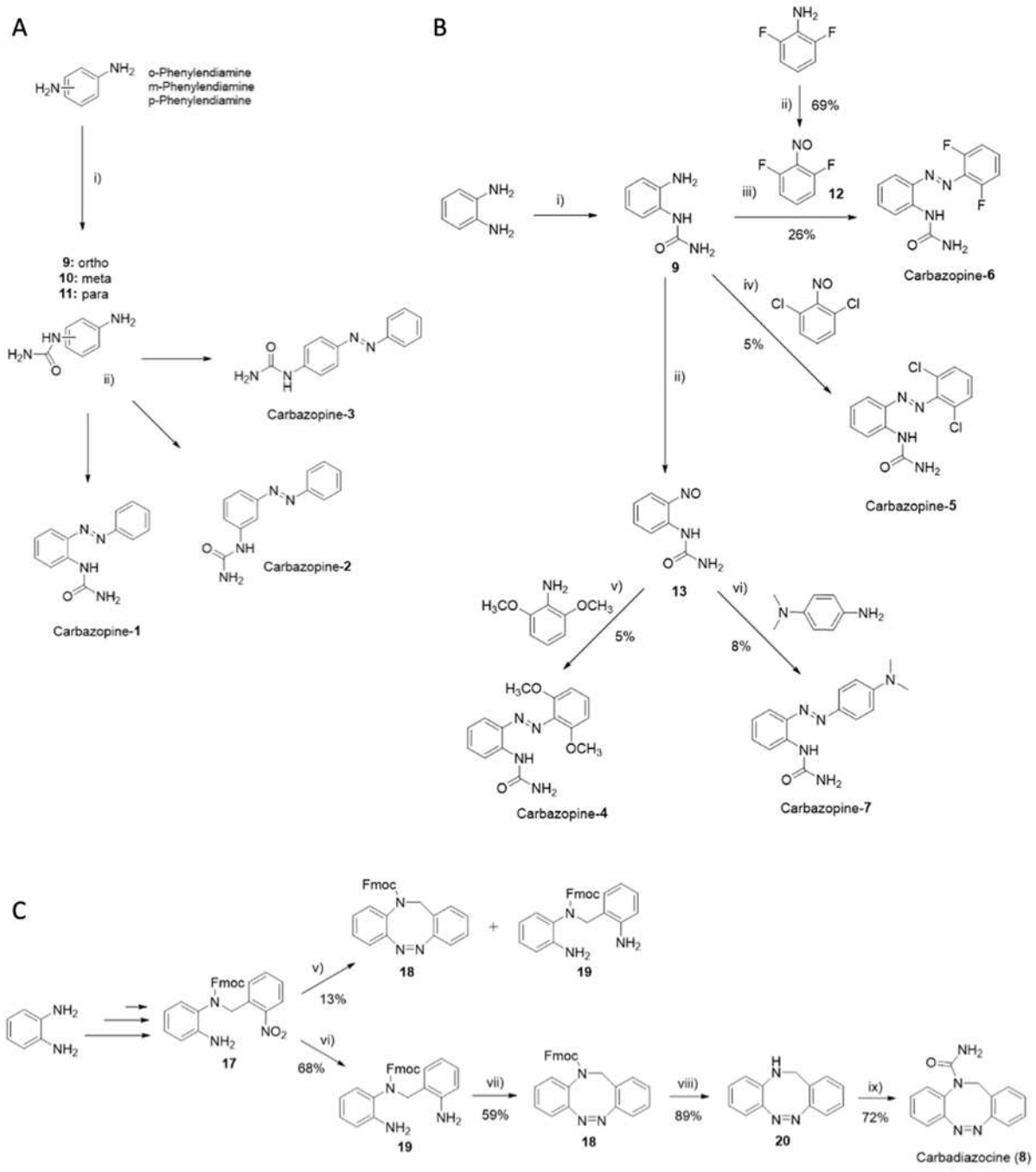

Scheme 1. Reaction conditions for: **A)** i) KCNO, AcOH/H_2O, 7 h, rt; ii) nitrosobenzene, AcOH, 5 h, rt; **B)** i) KCNO, AcOH/H_2O, 8 h, rt; ii) oxone, DCM/H_2O, 1 h, rt; iii) AcOH, 48 h, rt; iv) AcOH, 72 h, rt; v) AcOH, 48 h, rt to 40 °C; vi) AcOH, 15 h, rt; **C)** (v) 1.) Zn powder, NH_4Cl, EtOH, 10 min, 70 °C; 2.) $FeCl_3$ 6 H_2O, 15 min, 0 °C; 3.) AcOH, 17 h, rt; (vi) Zn powder, NH_4Cl, EtOH, 1 h, 70 °C (vii) oxone, AcOH, 18 h, rt; (viii) Et_3N in DCM (50%), 24 h, rt; (ix) 1.) Triphosgene, Et_3N, toluene, 8 h, rt; 2.) NH_4OH 30%, 18 h, rt.

to afford the *ortho* halogen di-substituted products Carbazopine-**5** and –**6**. The synthesis of the nitroso compounds **12** and **13** was achieved by oxidation with oxone in a biphasic system of water (H_2O) and dichloromethane (DCM). The intermediate **13** was isolated after extraction of the organic phase without further purification and it was directly combined in acetic acid (AcOH) with 2,6-dimethoxyaniline and *N*,*N*-Dimethyl-1,4-phenylenediamine to provide the respective final products Carbazopine-**4** and –**7**. The Mills reaction could only take place when the amino group was held in the most electron-rich aromatic ring, while the oxidation to the nitroso intermediate was favored in electron-poor aromatic rings. The azo coupling for all the substituted analogs (**4**–**7**) gave low yields (between 5–8%), possibly due to steric hindrance of the *ortho* substituents. Indeed, a moderately better yield (26%) was achieved for

compound **6** bearing two fluorine atoms, comparable in size to hydrogen atoms.

Finally, the synthesis of the *N*-bridged diazocine Carbadiazocine (**8**) followed a reported synthetic Scheme with minor modifications (SI, Scheme S3)[40] and the addition of the final *N*-substitution with the urea moiety (Scheme 1C). For instance, the yield for the *Fmoc* protection of the amino group was consistently improved (from 47 % to 94 %) using anhydrous 1,4-dioxane as solvent instead of the reported dry dimethylformamide (DMF), (SI, Scheme S3). The key step for ring closure and formation of the N-bridged diazocine ring gave a poor yield (13 %) compared to the reported one (40 %), mainly due to the formation of the side product **19**. Since this side product results from excessive reduction of the nitro group, we tried to limit the exposure time to zinc/NH_4Cl from 10 minutes to 5 minutes. However, the final yield did not change. To overcome this limitation, an additional step was introduced to fully convert compound **17** into the di-amine product **19**: the same conditions were retained, but the reaction was stirred for 1 hour, thus allowing the formation of the desired product **19** in 68 % yield. The intramolecular azo coupling for the ring closure of **19** was carried out in glacial acetic acid with either mCPBA (32 % yield) or oxone, which provided the diazocine **18** in 59 % yield.

The final carboxamination of the NH-diazocine **20** was not feasible using isocyanate in acidic conditions due to the reported tautomerization to the imine bridged hydrazine.[40] Therefore, we used triphosgene in the presence of triethylamine (Et_3N) to form the acyl chloride intermediate, followed by the addition of aqueous ammonia (NH_3) 30 %[41] to provide the urea-substituted final product Carbadiazocine (**8**) in 72 % yield. The chemical characterization of every intermediate is reported in the Supporting Information file.

Photochemical Characterization of Carbamazepine Azobenzene and Diazocine Analogs

The photochemical properties of the synthesized compounds were characterized using UV/Vis spectrophotometry. We measured the ability of the molecules to efficiently isomerize and change their absorption spectra upon illumination and during thermal relaxation in the dark. All the linear compounds (Carbazopine-**1** to −**7**) showed the typical absorption bands of azobenzene (photochemical behavior described in SI, see Figures S12–S19). The % of *trans* isomers at the photostationary states (PSS) was quantified by HLPC analysis at the isosbestic point (SI, Figures S20–S25). The amount of Carbazopine-**1** *trans* isomer changed from 98 % in the dark-adapted state to a minimum of 22 % upon irradiation with 380 nm light (Figure 2ABC and Supporting Information Figures S12, S20 for absorption and HPLC measurements, respectively). Reverse switching from *cis* to *trans* can be obtained by irradiation at 500 nm and yields a maximum of 47 % *trans* isomer due to the overlap of the nπ* absorption band between the two isomers. Complete back-isomerization of Carbazopine-**1** can be achieved by spontaneous thermal relaxation in dark conditions with a half-life of $t_{1/2} = 3.6$ h (SI, Figure S12C).[18,42,43]

In contrast to the linear azobenzenes, Carbadiazocine (**8**) is thermodynamically stable in its *cis* form as other diazocines.[8,40,44] The absorption maximum of dark-adapted Carbadiazocine can be excited at 400–420 nm to achieve a mixture of 49 % *cis* and 51 % *trans* (Figure 2DEF and Supporting Information Figures S19 and S25). Interestingly, the distance between the *cis* and *trans* nπ* absorption bands allows for selective excitation of the *trans* isomer using wavelengths longer than 500 nm and achieving complete back-isomerization to the *cis* form. Quantitively recovering the dark-adapted configuration is a desirable feature as it allows to have fully reversible control over the activation and deactivation of the drug. Wavelengths in the 500–600 nm range also allow reducing toxicity and increasing tissue penetration compared to UV light. Hence, we irradiated 50 μM *trans* Carbadiazocine (**8**) using a 590 nm LED (120 mW, see SI) and observed quantitative conversion to the *cis* isomer in 45 min (Figure 2EF). Full conversion can be conveniently achieved in 1 min using a common halogen lamp (fiber optic gooseneck illuminator for surgery or microscopy, Supporting Information Figure S19F). The thermal relaxation half-life in the dark of *trans*-enriched Carbadiazocine (**8**) is $t_{1/2} = 2.2$ h (SI Figure S19C), which offers a time window to test separately *cis*-relaxed and *trans*-enriched solutions in biological assays.

The photoisomerization of all the synthesized molecules is reversible and repeatable for several cycles of illumination without apparent loss in absorption or any evidence of degradation. The results of the photochemical characterization are outlined in Supporting Information and summarized in Table S3–S4 for the entire compound library and for Carbazopine-**1** and Carbadiazocine (**8**).

Carbazopine-1 and Carbadiazocine (8) Reversibly Photocontrol Neuronal Firing in vitro

To identify active and photoswitchable carbamazepine analogs, we screened them using calcium imaging in cultured hippocampal neurons (see methods in SI). We looked for alterations in spontaneous calcium activity upon applying each compound in the dark, and under different illumination conditions to favor their *cis* and *trans* forms. Among the five linear compounds that are soluble in water with less than 1 % DMSO (Table S3), we found that only Carbazopine-**1** inhibits neuronal activity in a light-dependent manner (Figure 3 and Supporting Information Figure S26), while the others do not show clear effects.

We further characterized the ability of Carbazopine-**1** to photocontrol neuronal activity by directly measuring the frequency of action potential generation using patch clamp electrophysiology (Figure 3). At 30 μM, Carbazopine-**1** in the dark or under 500 nm light robustly decreases the firing frequency from 3.6 Hz to 0.4 Hz, and 380 nm illumination readily reverts this effect and restores firing in a few seconds (Figure 3A). The effects of 380 nm and 500 nm illumination during Carbazopine-**1** application were repeatable, as shown

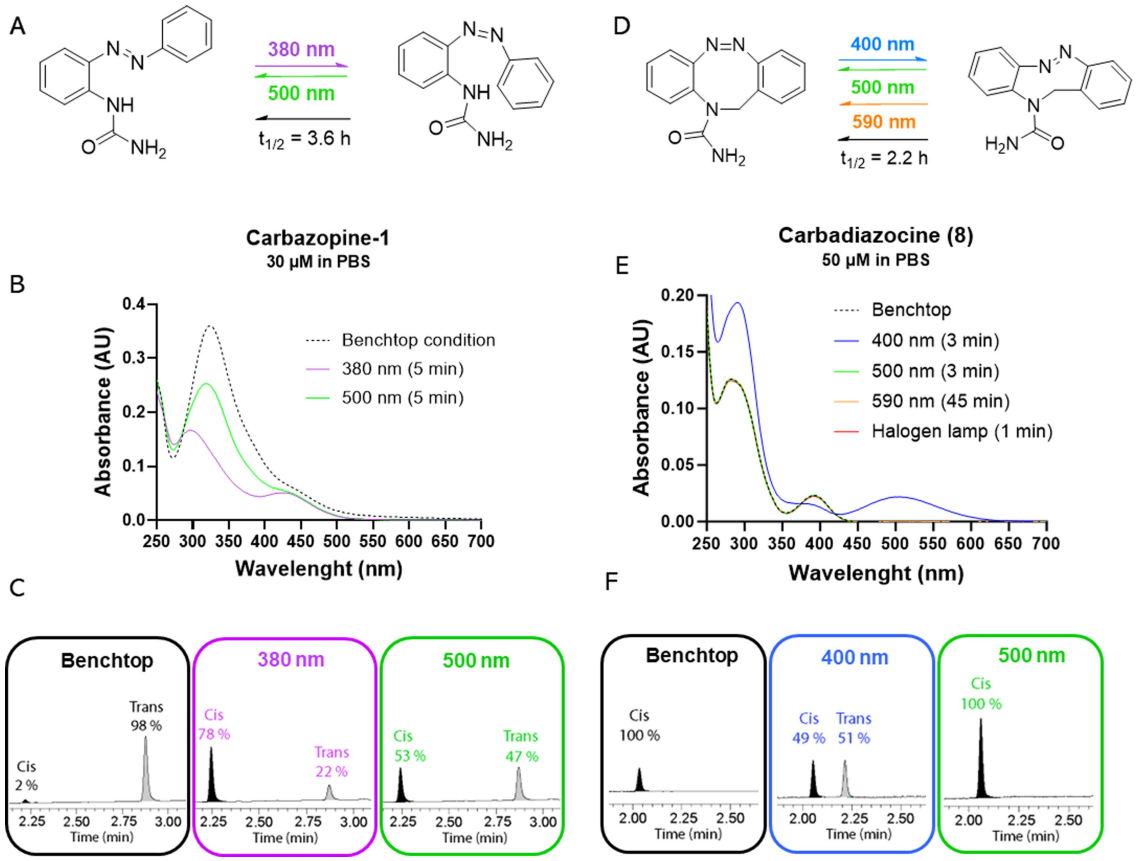

Figure 2. Photochromic properties of selected photoswitchable analogs of carbamazepine. **A)** Carbazopine-**1** can be isomerized under 380 nm illumination to a maximum of 78 % *cis*, and under 500 nm to a maximum of 47 % *trans*. Thermal relaxation in the dark back-isomerizes Carbazopine-**1** to 98 % *trans* in $t_{1/2} = 3.6$ h. **B)** Absorption spectra after the illumination conditions discussed in A. **C)** HPLC chromatograms showing the quantification of the photostationary states (PSS) after the illumination at the selected wavelengths (380 nm–500 nm). **D)** Carbadiazocine (**8**) can be isomerized using 400 nm illumination to a maximum of 51 % *trans*, and to 100 % *cis* with 500 nm (3 min), 590 nm (45 min), and halogen lamp light (1 min). Thermal relaxation in the dark back-isomerizes Carbadiazocine (**8**) to 100 % *cis* in $t_{1/2} = 2.2$ h. **E)** Absorption spectra after the illumination conditions discussed in C. **F)** HPLC chromatograms showing the quantification of the photostationary states (PSS) after the illumination at the selected wavelengths (400 nm–500 nm).

in the example recording and the firing frequency quantification below. On average, 30 µM of Carbazopine-**1** under 500 nm light decreased the firing frequency to 8 ± 5 % relative to the control ($P < 0.001$, $n = 6$), while 380 nm light induced a recovery up to 61 ± 27 % ($P < 0.05$, $n = 6$). This control of neuronal firing with light is concentration-dependent: 10 µM Carbazopine-**1** does not induce statistically significant changes in relative firing frequency (120 ± 54 % under 500 nm light and 108 ± 27 % under 380 nm light, $n = 5$), whereas at 50 µM it blocks neuronal firing regardless of the illumination conditions (0 %, $n = 3$ under 500 nm and 7 ± 12 %, $n = 3$ under 380 nm). Thus, 30 µM is the optimal concentration of Carbazopine-**1** to photocontrol neuroinhibition *in vitro*. However, it is active in the dark and deactivated under violet light, which is a limitation to producing localized drug photoactivation.

We then tested the neuronal activity of Carbadiazocine (**8**) using the same assay. Figure 3C shows an example of current clamp recording and the corresponding quantification of the firing frequency. At 30 µM in the dark, Carbadiazocine (**8**) decreases the firing frequency to 72 ± 5 % compared to control conditions ($P > 0.05$; Figure 3CD), and under 400 nm light, it decreases to 28 ± 13 % ($P < 0.01$; $n = 4$). This effect is reversible under 500 nm light and repeatable when illuminating again with 400 and 500 nm. The efficient and reversible modulation of action potential generation by hippocampal neurons indicates that Carbadiazocine (**8**) is a light-activated photoswitchable neuroinhibitor at a concentration of 30 µM *in vitro*. It is thus complementary to Carbazopine-**1** and constitutes another good candidate to produce localized neuroinhibition with light.

Carbazopine-1 and Carbadiazocine (8) Reversibly Photocontrol Zebrafish Larvae Behavior

The photoswitchable derivatives of carbamazepine displaying activity *in vitro* (Figure 3) were further evaluated *in vivo* in zebrafish (*Danio rerio*) larvae at early developmental stage (7 days post fertilization, dpf) using a high-throughput behavioral assay.[15] Compounds were diluted in zebrafish water and freely swimming larvae were incubated for 20 min

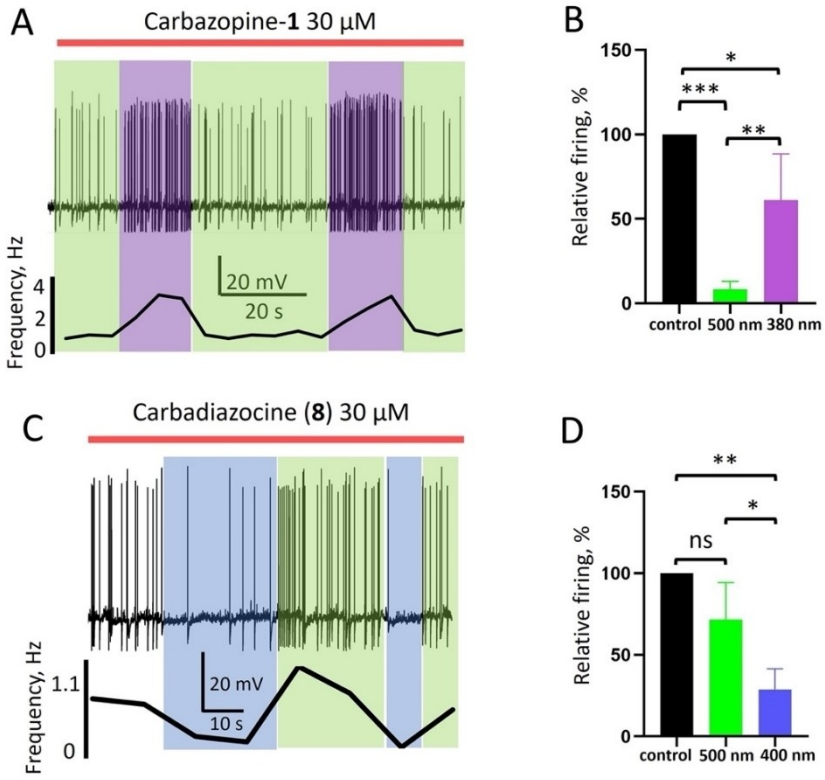

Figure 3. Photoswitchable carbamazepine analogs photocontrol action potential firing *in vitro*. **A)** Representative current clamp recording showing photocontrol of the spontaneous firing frequency in cultured hippocampal neurons by 30 µM Carbazopine-**1**. The red bar indicates the duration of Carbazopine-**1** application, green and violet boxes indicate periods of 500 nm and 380 nm illumination, respectively. A graph below the trace shows the frequency of action potential (AP) generation for each condition, calculated from the number of AP fired in 10 s time intervals. **B)** Quantification of the effect of 30 µM Carbazopine-**1** on the relative firing frequency during illumination with green or violet light in correspondence to the column color ($n=6$ cells, *-$P<0.05$; **-$P<0.01$; ***-$P<0.001$). Error bars indicate standard deviation (S. D.) **C)** Representative current clamp trace showing photocontrol of neuronal firing by 30 µM Carbadiazocine (**8**). The red bar indicates application of the compound, green and blue boxes indicate periods of 500 nm and 400 nm illumination, respectively. The calculated firing frequency is shown below. **D)** Quantification of neuroinhibition by 30 µM Carbadiazocine (**8**) during illumination with green or violet light in correspondence to the column color ($n=4$ cells, *-$P<0.05$; **-$P<0.01$; ns—not significant). Error bars indicate S. D.

to allow drug uptake[15,45] prior to analyzing their behavior under varying light conditions applied during the experiment (Figures 4 and 5 and SI). Carbazopine-**1** at high concentrations (50–100 µM, red and green traces in Figure 4A top) transiently increased the swum distance during the initial relaxation period (RP) in the dark (0–20 min, shaded grey) in comparison to vehicle (black trace). Vehicle-treated larvae display a characteristic swimming response to 380 nm UV light (avoidance).[46,47] This behavior is blocked by Carbazopine-**1** in a light-dependent manner (absence of swimming during UV periods and restoration under 500 nm green light). The statistical analysis for groups of 12—24 larvae is shown in Figure 4A bottom. Overall, Carbazopine-**1** induced a dose-dependent, reversibly photoswitchable effect on the ability of larvae to swim. The compound appears to induce activity in *trans* compared to vehicle. Since the time course of the responses of Figure 4A top is masked by the kinetics of drug uptake and action, and by natural responses to light, we repeated the experiments with blinded larvae (treated with high intensity light, see Supporting Information methods and reference[23]). Blinded larvae display reduced behavioral reactions to light changes but continue to react to mechanical (touch-evoked responses) and vibrational stimuli. We observed lower RP activity and photoresponses in vehicle-treated blind larvae while in 50 µM Carbazopine-**1** the dark activity and photoresponses to 380/500 nm light were maintained (Figure 4B displays activity traces in the top panel and quantification in the bottom). These experiments are exemplified in the Supporting Information Movie M1. As a qualitative assessment of toxicity, we kept larvae in Carbazopine-**1** for 24 h after the experiments, and we noticed that all fish larvae were dead at 100 µM dose.

Carbadiazocine (**8**) also produced a dose- and light-dependent effect on swimming behavior (Figure 5). During the initial dark RP, no significant effect of the drug compared to the vehicle was observed but subsequent illumination produced robust and reversible photoresponses at 10–50 µM Carbadiazocine (**8**). In the absence of drugs and under constant visible wavelengths, such as 420 and 500 nm, intact zebrafish larvae do not show anxiety-related behaviors,[48,49] displaying scoot swimming and sporadic darting behaviors.[50] Changes in wavelength within this range elicit negligible responses (see Figure 5A, top panel,

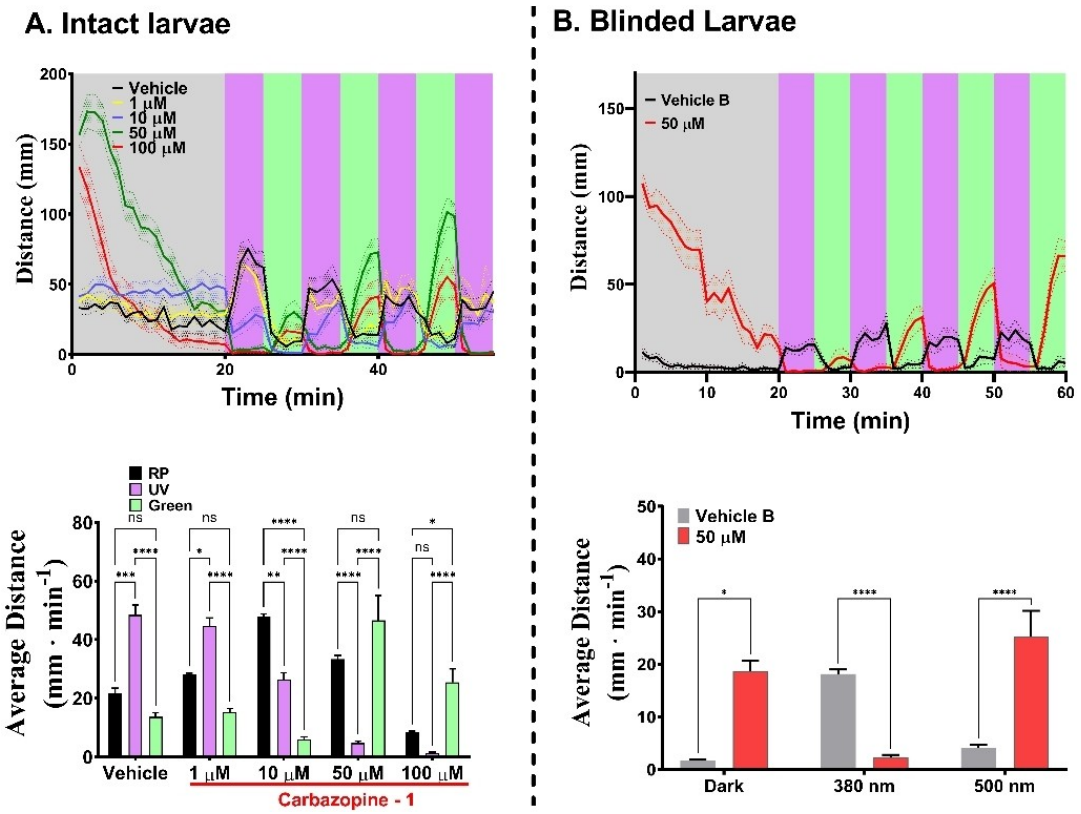

Figure 4. Behavioral characterization of Carbazopine-**1** in 7 days post-fertilization (dpf) Tupfel-Long zebrafish larvae. **Panel A, top**. Swimming activity (mm per min) trajectories for vehicle (1% DMSO, $n=10$ larvae, black trace) and Carbazopine-**1** treated larvae (1 µM, yellow trace, $n=12$; 10 µM, blue trace, $n=24$; 50 µM, red trace, $n=23$; and 100 µM, $n=21$, green trace). Larvae were exposed to an initial 20 min darkness period (relaxing period, RP) in the presence of vehicle or drug (dark relaxed *trans* isoform). Illumination periods were alternated every 5 min to isomerize the drug between its *trans* state (500 nm, green shaded bands) and *cis* state (380 nm UV, purple shaded bands). Patterned bands around traces represent the S.E.M. for each group of larvae. **Panel A, bottom**. Quantification of the average distance swum by each group over 3 light cycles of UV and visible illumination wavelengths (minute 20 to 50). Error bars represent S.E.M. for a total of 15 min per light condition. **Panel B, top**. Swimming activity (mm per min) of blinded 7 dpf larvae treated with vehicle (1% DMSO, $n=12$, black trace) and 50 µM Carbazopine-**1** treated ($n=12$, red trace). Illumination conditions as in panel A. Patterned bands indicate S.E.M. per each group. **Panel B, bottom**. Quantification of the average distance swum by each group during 5 min of darkness (minute 15 to 20) and four 5-min cycles of 380 nm and 500 nm (20 min integrations). Two-way ANOVA with Tukey's multiple comparison test was performed were alpha = 0.05; $p<0.05$ = *, $p<0.0001$ = ****. Error bars represent S.E.M.

black vehicle trace between 20–55 min). However, switching the light off after a prolonged period of visible illumination triggers an enhanced photokinetic swimming behavior known as successive induction response[51,52] (Figure 5A top panel, black vehicle trace between minutes 55–60, 65–70, 75–80, and 85–90). In contrast to these native behaviors of untreated larvae, 10–50 µM Carbadiazocine (**8**) increases locomotion under 420 nm violet light and decreases it under 500 nm (green). These wavelengths isomerize the compound respectively to *trans* and back to *cis* (Figure 2). The effect is stronger but less reversible and repeatable at 50 µM (red traces in Figure 5A) probably due to exhaustion after the first cycles where treated larvae swum eight times more than in vehicle. Interestingly, light-off transitions (55–90 min) lead to smaller changes in locomotion (e.g. blue traces in Figure 5A) likely because the compound is thermally stable in the time frame of minutes after switching the light off ($t_{1/2}=2.2$ h, Figure 2). We also tested the effect on larval behavior of illumination with the halogen warm white lamp used for *trans-cis* isomerization of Carbadiazocine (**8**) (Figure 2). This is indicated by orange shaded bands in Figure 5A and it resulted in rapid and effective blockade of larval hyperactivity. The quantification and statistical analysis of these experiments in intact larvae are shown in the bottom panel of Figure 5A. Overall, Carbadiazocine (**8**) appears to be inactive in the dark compared to vehicle and elicits swimming behavior under violet illumination, which can be reversed with green or amber light. As in Figure 4, we aimed to isolate the drug effects by studying 10 µM Carbadiazocine (**8**) in blinded larvae (Figure 5B and SI). Vehicle treated animals show lower swimming activity and nearly absent photoresponses compared to intact ones. Behavioral photoresponses elicited by Carbadiazocine (**8**) are observed and statistically significant, with 420 nm light increasing locomotion and 500 nm light decreasing it. These experiments are exemplified in Supporting Information Movies M2 and M3. We also tested Carbadiazocine (**8**) toxicity qualitatively by keeping the larvae in their wells for

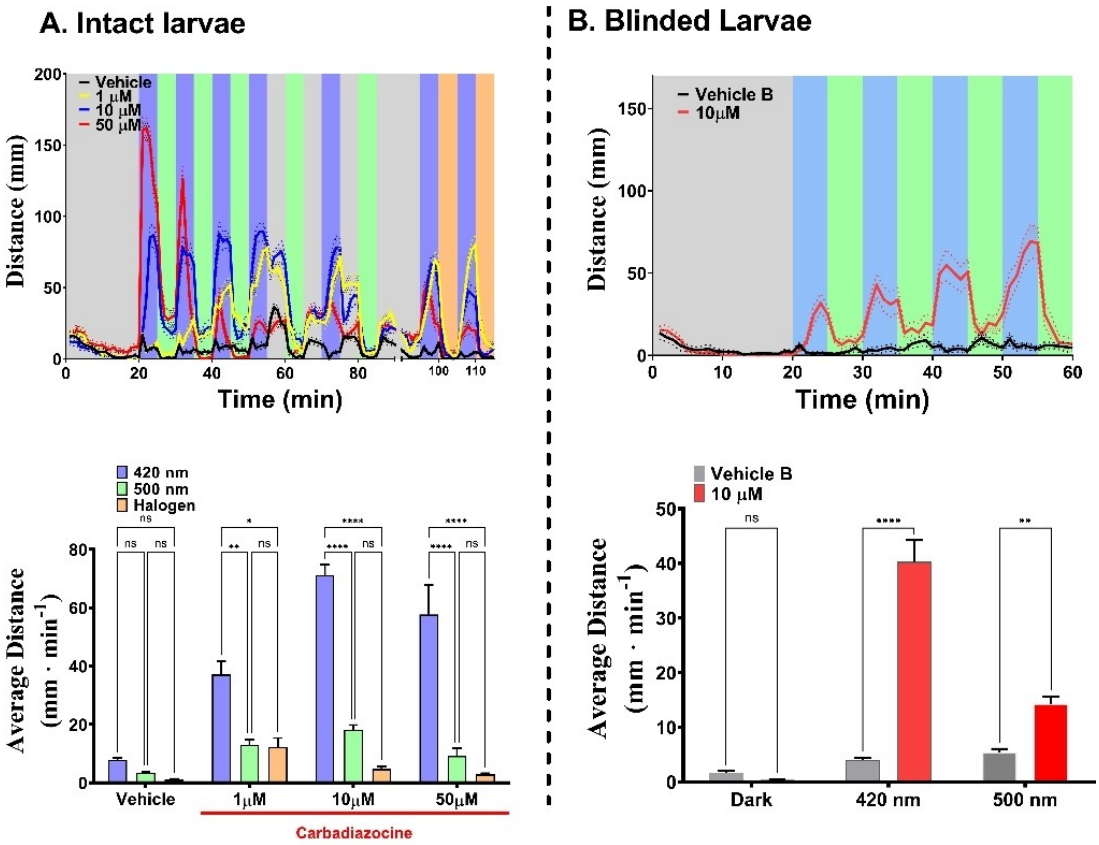

Figure 5. Behavioral characterization of Carbadiazocine (**8**) in 7 dpf zebrafish larvae. **Panel A, top**. Swimming activity (mm per min) trajectories for Vehicle (1% DMSO, black trace) and Carbadiazocine (**8**) treated larvae ($n=24$ per group) (1 μM, yellow trace; 10 μM, blue trace; 50 μM, red trace). Larvae were exposed to an initial 20 min darkness period in the presence of vehicle or drug (dark relaxed *cis* isoform). Illumination periods were alternated every 5 min to isomerize the drug between its *cis* state (500 nm or halogen warm white light, green and orange shaded bands, respectively) and *trans* state (420 nm, blue shaded bands). Patterned bands around traces represent the S.E.M. per each group of larvae ($n=24$). **Panel A, bottom**. Quantification of the average distance swum by each group over all light cycles of 420 nm (25 min integration), 500 nm (25 min) and halogen lamp (10 min). **Panel B, top**. Swimming activity (mm per min) of blinded 7 dpf larvae treated with vehicle (1% DMSO, black trace, $n=12$) and 10 μM Carbadiazocine (**8**) (red trace, $n=12$). Larvae were exposed to varying light conditions with a first 20 min of darkness and 5 min alternating cycles of 420 nm and 500 nm light. Patterned bands depict S.E.M. per each group. **Panel B, bottom**. Quantification of the average distance swum by each group over 5 min of dark (between minutes 15–20) and over all 5 min light cycles of 420 nm and 500 nm (20 min integrations). Two-way ANOVA with Tukey's multiple comparison test was performed were alpha = 0.05; $p<0.05$ = *, $p<0.0001$ = ****. Error bars represent S.E.M.

24 h after the assays, and we did not observe dead larvae at any concentration.

These results show that Carbazopine-**1** and Carbadiazocine (**8**) enable robust and reversible photocontrol of wild-type zebrafish larvae behavior, and the latter does not produce apparent toxicity in the studied concentration range.

Carbadiazocine (8) Enables Non-Invasive Photocontrol of Neuropathic Pain in Rats

The favorable molecular properties of Figures 2 and 3 and the photocontrol in zebrafish larvae shown in Figures 4 and 5 prompted us to proceed with mammals. The neuroinhibition mediated by Carbazopine-**1** and Carbadiazocine (**8**) offers opportunities to demonstrate a proof of concept of photocontrolled analgesia, so we tested them using nociception assays in a rat model of neuropathic pain (chronic-constriction injury, CCI, Figure 6 and Supporting Information Figures S27–S28). Briefly, animals were cannulated for intrathecal (i.t.) drug administration, and chronic pain was induced surgically by CCI. Sensory threshold changes were determined using two nociceptive tests (von Frey mechanical test and acetone thermal test, see Supporting Information Figure S27B) in lesioned and control paws. In preliminary experiments with photoswitchable ligands of α-adrenergic receptors (adrenoswitches),[24] we observed partial inhibition of pain behavior upon i.t. injection of the drugs, albeit at concentrations too high to allow photoswitching (SI Figure S27E–H). We then injected either vehicle (10% DMSO), 65 μM carbamazepine, Carbamazopine-**1** (60 μM in preliminary experiments, see below) or Carbadiazocine (**8**) (200, 600 μM) and performed nociceptive tests (Figure 6A and Supporting Information Figure S28). Carbamazepine induced significant analgesic effects (increase of the mechan-

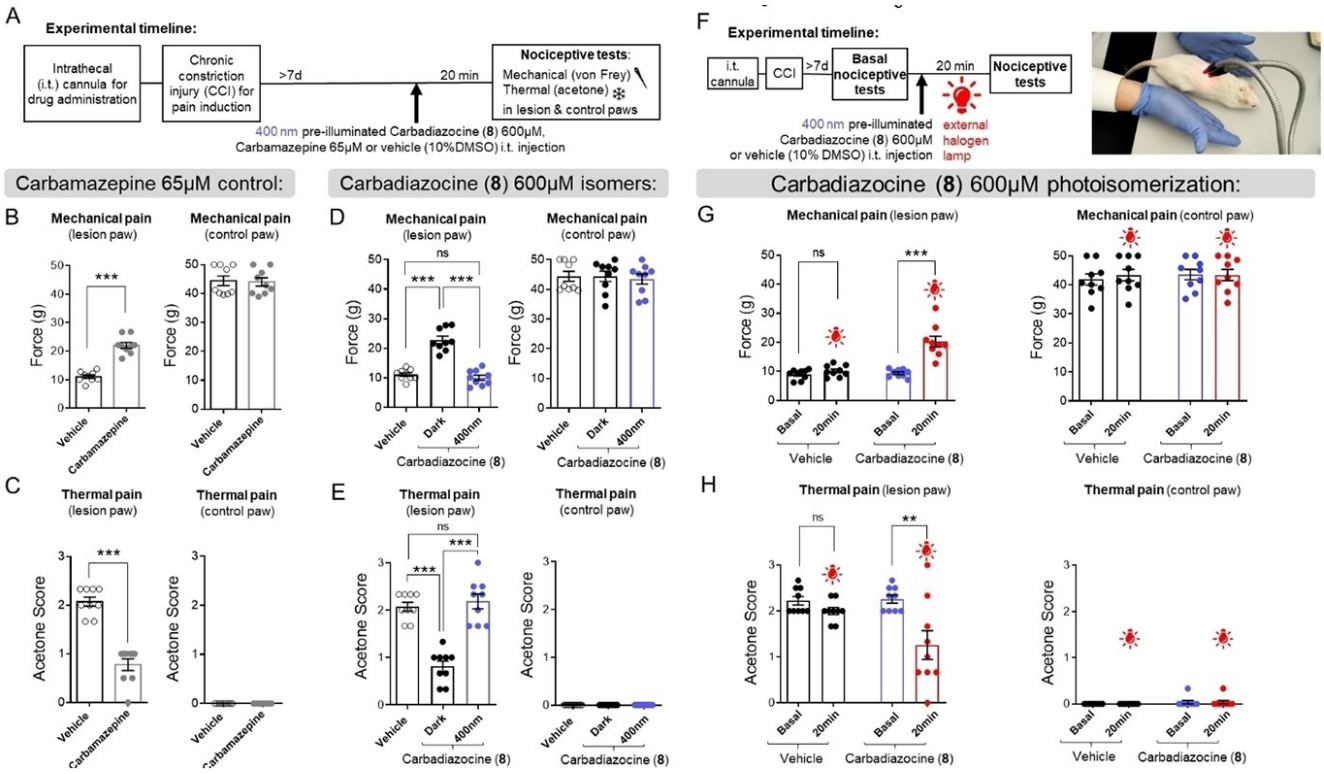

Figure 6. Effect of Carbadiazocine (**8**) in a rat model of pain. (**A**) Animals were cannulated for intrathecal (i.t) drug administration and chronic pain-like behavior was induced surgically by lesioning one paw using CCI. After at least 7 days, animals were injected i.t. with either vehicle (10% DMSO) or treatments and 20 min afterwards they were subject to the nociceptive tests (see Supporting Information Figure S27–S28). (**B**) Injection of 20 µl carbamazepine (65 µM) as positive control. Von Frey test (mechanical pain-like behavior) measured the withdrawal threshold (force, g) in the lesioned and control paws of each animal (left and right panels, respectively, N = 9). Carbamazepine increased the withdrawal threshold in the lesioned paw, indicative of analgesia (see time course in Figure S28C). (**C**) Acetone score (thermal pain-like behavior) was reduced in the lesioned paw after carbamazepine i.t. injection (N = 9), confirming the analgesic effect (see time course in Figure S28D). (**D**) Injection of 20 µl of both dark-relaxed and 400 nm-preilluminated Carbadiazocine (**8**) (600 µM, black and violet dots, respectively, N = 9 each). Dark-relaxed **8** increased the withdrawal threshold in the lesioned paw compared to the preilluminated form and to the vehicle, indicative of analgesia. No effects were observed in the control paw. (**E**) Dark-relaxed **8** also reduced the acetone score (thermal pain-like behavior) compared to the preilluminated form and to the vehicle (N = 9). The activity of preilluminated **8** was similar to that of the vehicle in either test. (**F**) Experiment timeline: recording of nociceptive tests for basal measurements prior to i.t. drug administration. Inactive 400 nm preilluminated Carbadiazocine (**8**) was then injected and the nociceptive tests were repeated after 20 min irradiation at the back of the animal (L4–L6) with a fiber optic dual gooseneck illuminator equipped with a halogen lamp. The animals remained still under the lamp, indicating pain relief. (**G**) Quantification of mechanical pain-like behavior in the lesioned paw showed no intrinsic effects of halogen light in the absence of the drug (black and red dots corresponding to vehicle injection) and increased the withdrawal threshold between preilluminated **8** before and after illumination with the halogen lamp through the fur and skin (violet and red dots, respectively). (**H**) Thermal pain-like behavior was also lower in the lesioned paw upon illuminating the back of the animal injected with preilluminated **8** and was unaltered in the control paw regardless of the presence of the drug or the illumination. Two-tailed unpaired Student's T test was used to compare the values between the two groups and One-way ANOVA with Tukey's multiple comparison test was performed between more than two groups; $p < 0.01$ = **, $p < 0.001$ = ***. Error bars represent S.E.M.

ical withdrawal threshold and decrease of the acetone score only in the lesioned paw, Figure 6BC), in agreement with reported results.[53] The corresponding time courses are shown in Supporting Information Figure S28CD.

Injection of Carbazopine-**1** induced notable side effects in rats, including reduced spontaneous motor activity, back-arching, twitching, closed eyes, and vocalizations. Due to these adverse reactions, further testing of Carbazopine-**1** was not pursued in this study. In contrast, both isomers of Carbadiazocine (**8**) at a concentration of 600 µM were well tolerated, showing no apparent signs of anesthesia, sedation, or notable alterations in behavior, and were thus studied in detail. The mechanical and thermal pain were assessed after i.t. injection of 600 µM dark-relaxed and 400 nm pre-illuminated Carbadiazocine (**8**) (black and blue dots, respectively, in Figure 6DE). Dark-relaxed Carbadiazocine (**8**) induced significant analgesic effects, both in mechanical and thermal assays and only in the lesioned paw, not in the control paw. In contrast, the activity of preilluminated Carbadiazocine (**8**) was not significantly different from that of the vehicle in either test. The corresponding time courses are shown in Supporting Information Figure S28C–F.

These promising results suggested that it might be possible to photoinduce on-demand, spinal-mediated analgesia by injecting the inactive preilluminated Carbadiazocine (**8**) and using an external halogen lamp to non-invasively

isomerize it, taking advantage of the ability of the compound to isomerize under 590 nm light (Figure 2 and 5). Strikingly, when we performed this experiment, the animals remained still under the lamp, a behavior that suggested readily perceptible pain relief (Figure 6F and Supporting Information Movie M4). Detailed quantification of nociceptive tests confirmed significant analgesic effects of illumination, only in the lesioned paw and in the presence of Carbadiazocine (**8**) (Figure 6GH). Further studies are warranted to confirm the absence of side effects associated with local administration of Carbadiazocine (**8**) in the spinal cord. These investigations would provide valuable insights into the safety and efficacy of this approach, further informing its potential application in clinical settings.

We discuss below the major results of the article and their advantages and limitations compared to previously reported results (more detailed discussion can be found in the SI).

Our integral drug design involved (1) selecting protein targets validated for pain and epilepsy (α-adrenoceptors, Na_V channels), (2) choosing a clinically prescribed drug as a parent compound to obtain drug-like photoswitchable analogs, and (3) retaining only those analogs that can be used *in vivo* and that allow future optimization of their properties (including safety, ADMET, and formulation). The absence of activity of *meta* and *para* analogs (**2**, **3**) further validates the concept demonstrated with active *ortho* cryptoazologs (**1**) for tricyclic drugs.[22] In addition, we reported the first instance of diazocine crypoazalog (**8**) retaining the original tricyclic structure. Using halogen lamps and violet LEDs, the compound allows *in vivo* photoswitching of analgesia for neuropathic pain in rats with non-invasive illumination. Future improvements may afford bi-directional quantitative switching and lead to even stronger differences in firing rate with light.

The surprising differences in photoswitch sign between *in vitro* and *in vivo* assays can be attributed to the contributions of both excitatory and inhibitory neurons and to the complex effects of carbamazepine derivatives on conductance and gating mechanisms (activation and inactivation).[54,55] Note also that the three-dimensional geometry of diazocines (whose side ring planes adopt an angle of ~80° in *cis* and ~180° in *trans*)[56] differs from that of carbamazepine (~130°).[37] The angle of linear *cis* azobenzene ranges between 60°–90° depending on the substitutions.

Both Carbazopine-**1** and Carbadiazocine (**8**) retain the *in vitro* potency of carbamazepine and other AEDs (tens of μM)[57] and the latter does not show *in vivo* toxicity. Carbadiazocine (**8**) is less active in rats upon violet illumination (50 % *trans*-like) and converts quantitatively to 100 % *cis* with either green or orange light, the latter allowing deeper tissue penetration. Thus, doubling the concentration of the active isomer of Carbadiazocine (**8**) suffices to produce analgesic effects, probably because small changes in membrane potential near the firing threshold have large effects in neuronal activity. Carbadiazocine (**8**) is a small, drug-like, and water-soluble molecule that may retain the favorable characteristics of carbamazepine, including oral bioavailability and permeation through the blood–brain barrier. Taken together, our approach has overcome several hurdles to develop a photoswitchable AEDs with properties matching those of conventional drugs and allowing the use of non-invasive illumination in rats. Potential uses include the inhibition of pain signaling, seizures, and bipolar disorder.

The development of photoswitchable ligands of ion channels involved in neuronal excitability has largely focused on potassium channels,[58] with fewer photoswitches targeting sodium channels,[59] despite their unique role in action potential generation. Sustained efforts to develop photoswitchable AEDs and other drugs should lead to treatments offering highly localized and on-demand neuroinhibitory efficacy without systemic adverse effects.

Conclusions

To meet the need for AEDs that inhibit nerve signals under spatiotemporal control, we have developed photoswitchable analogs of carbamazepine. For that purpose, we expanded our method of azologization of tricyclic drugs to *meta*/*para* cryptoazologs (including different substitutions) and to diazocine cryptoazologs. Our results allowed validation of the concept of *ortho* cryptoazologs (uniquely exemplified by Carbazopine-**1**) and gave rise to Carbadiazocine (**8**). This compound offers promising drug-like properties and effective analgesia *in vivo* against neuropathic pain without signs of anesthesia, sedation or toxicity, and a simple and compelling treatment demonstration with non-invasive illumination.

Acknowledgements

The authors wish to thank José Antonio García-Partida for his excellent technical assistance and Nayeli Pérez-Pérez, Josep Pous, Adrià Tauste, Adrián Valls-Carbó, Enric Carbonell, and Joaquín Martínez-Tambella for useful discussions. This research has received funding from the European Union's HORIZON-EIC-2023 PATHFINDER-OPEN-01 programme under grant agreement No. 101130883; from the European Union′s Horizon 2020 programme (the Human Brain Project SGA3, 945539 and DEEPER, 101016787); project DEEPRED with reference PID2019-111493RB-I00 funded by MICIU/AEI /10.13039/501100011033; project EPILLUM with reference PID2022-142609OB-I00 funded by MICIU/AEI /10.13039/501100011033 and by FEDER, UE; "la Caixa" foundation (ID 100010434, agreement LCF/PR/HR19/52160010); SGR-Cat 2021 with reference 2021 SGR 01410 (AGAUR, Generalitat de Catalunya); Research Network in Biomedicine eBrains-Spain, RED2022-134823-E; the CIBERSAM (CB07/09/0033), the Junta de Andalucía (Consejería de Transformación Económica, Industria, Conocimiento y Universidad, grant CTS-510), and the Instituto de Investigación e Innovación en Ciencias Biomédicas de Cádiz-INiBICA (grant IN-CO9). IBEC is a recipient of the Severo Ochoa Award of Excellence from MICIU. G. M. was supported by

a Ramón y Cajal Investigator grant (RYC2021-033056-I financed by MCIN/AEI /10.13039/501100011033 and by European Union NextGeneration EU/PRTR). All experiments on animals were conducted in compliance with EU directive 2010/63/EU and Spanish guidelines (Laws 32/2007, 6/2013, and RD 53/2013) and were authorized by the Barcelona Biomedical Research Park (PRBB) Animal Research Ethics Committee and the local government (code #9891), by Parc Científic de Barcelona (21-000-PG), and by the Committee for Animal Experimentation at the University of Cádiz (Spain) (10/10/2023/086).

Conflict of Interest

Some of the authors have submitted a patent application covering these compounds, as stated in the main text of the article.

Data Availability Statement

The datasets generated and analyzed during the current study are available from the corresponding author on reasonable request. Some of the authors disclose that they have filed a patent application covering compounds included in this article.

Keywords: azobenzene · diazocine · tricyclic drugs · photopharmacology · neuromodulation · pain · epilepsy

[1] M. A. Raji, *Lancet Oncol.* **2005**, *6*, 357.
[2] T. S. Jensen, *Eur. J. Pain* **2002**, *6*, 61–68.
[3] E. C. Emery, G. T. Young, E. M. Berrocoso, L. Chen, P. A. McNaughton, *Science (1979)* **2011**, *333*, 1462–1466.
[4] A. Ortega-Álvaro, E. Berrocoso, R. Rey-Brea, J. C. Leza, J. A. Mico, *Life Sci.* **2012**, *90*, 13–20.
[5] L. Colloca, T. Ludman, D. Bouhassira, R. Baron, A. H. Dickenson, D. Yarnitsky, R. Freeman, A. Truini, N. Attal, N. B. Finnerup, *Nat Rev Dis Primers* **2017**, *3*.
[6] M. Selim, A. C. Anilkumar, E. Cichowski, in *StatPearls [Internet]*, StatPearls Publishing **2023**.
[7] P. Kobauri, F. J. Dekker, W. Szymanski, B. L. Feringa, *Angew. Chem.* **2023**, e202300681.
[8] A. Mukherjee, M. D. Seyfried, B. J. Ravoo, *Angew. Chem. Int. Ed.* **2023**, *62*, e202304437.
[9] P. Bregestovski, G. Maleeva, P. Gorostiza, *Br. J. Pharmacol.* **2018**, *175*, 1892–1902.
[10] F. A. Peralta, M. Balcon, A. Martz, D. Biljali, F. Cevoli, B. Arnould, A. Taly, T. Chataigneau, T. Grutter, *Nat. Commun.* **2023**, *14*, 1269.
[11] A. Garrido-Charles, A. Huet, C. Matera, A. Thirumalai, J. Hernando, A. Llebaria, T. Moser, P. Gorostiza, *J. Am. Chem. Soc.* **2022**, *144*, 9229–9239.
[12] G. Maleeva, A. Nin-Hill, K. Rustler, E. Petukhova, D. Ponomareva, E. Mukhametova, A. M. J. Gomila, D. Wutz, M. Alfonso-Prieto, B. König, *eNeuro* **2021**, *8*.
[13] K. Rustler, G. Maleeva, A. M. J. Gomila, P. Gorostiza, P. Bregestovski, B. König, *Chem. Eur. J.* **2020**, *26*, 12722–12727.
[14] G. Maleeva, D. Wutz, K. Rustler, A. Nin-Hill, C. Rovira, E. Petukhova, A. Bautista-Barrufet, A. Gomila-Juaneda, P. Scholze, F. Peiretti, *Br. J. Pharmacol.* **2019**, *176*, 2661–2677.
[15] A. M. J. Gomila, K. Rustler, G. Maleeva, A. Nin-Hill, D. Wutz, A. Bautista-Barrufet, X. Rovira, M. Bosch, E. Mukhametova, E. Petukhova, *Cell Chem. Biol.* **2020**, *27*, 1425–1433.
[16] L. Peverini, K. Dunning, F. A. Peralta, T. Grutter, *Curr. Opin. Pharmacol.* **2022**, *62*, 109–116.
[17] L. Yue, M. Pawlowski, S. S. Dellal, A. Xie, F. Feng, T. S. Otis, K. S. Bruzik, H. Qian, D. R. Pepperberg, *Nat. Commun.* **2012**, *3*, 1095.
[18] R. Castagna, G. Maleeva, D. Pirovano, C. Matera, P. Gorostiza, *J. Am. Chem. Soc.* **2022**, *144*, 15595–15602.
[19] A. Duran-Corbera, M. Faria, Y. Ma, E. Prats, A. Dias, J. Catena, K. L. Martinez, D. Raldua, A. Llebaria, X. Rovira, *Angew. Chem. Int. Ed.* **2022**, *61*, e202203449.
[20] F. Riefolo, C. Matera, A. Garrido-Charles, A. M. J. Gomila, R. Sortino, L. Agnetta, E. Claro, R. Masgrau, U. Holzgrabe, M. Batlle, *J. Am. Chem. Soc.* **2019**, *141*, 7628–7636.
[21] R. C. Sarott, A. E. G. Viray, P. Pfaff, A. Sadybekov, G. Rajic, V. Katritch, E. M. Carreira, J. A. Frank, *J. Am. Chem. Soc.* **2021**, *143*, 736–743.
[22] F. Riefolo, R. Sortino, C. Matera, E. Claro, B. Preda, S. Vitiello, S. Traserra, M. Jiménez, P. Gorostiza, *J. Med. Chem.* **2021**, *64*, 9259–9270.
[23] C. Matera, P. Calvé, V. Casadó-Anguera, R. Sortino, A. M. J. Gomila, E. Moreno, T. Gener, C. Delgado-Sallent, P. Nebot, D. Costazza, *Int. J. Mol. Sci.* **2022**, *23*, 10114.
[24] D. Prischich, A. M. J. Gomila, S. Milla-Navarro, G. Sangüesa, R. Diez-Alarcia, B. Preda, C. Matera, M. Batlle, L. Ramírez, E. Giralt, *Angew. Chem. Int. Ed.* **2021**, *60*, 3625–3631.
[25] J. Morstein, T. Bader, A. L. Cardillo, J. Schackmann, S. Ashok, J. L. Hougland, C. A. Hrycyna, D. H. Trauner, M. D. Distefano, *ACS Chem. Biol.* **2022**, *17*, 2945–2953.
[26] Y. Zhang, S. Peng, S. Lin, M. Ji, T. Du, X. Chen, H. Xu, *Bioorg. Med. Chem.* **2022**, *72*, 116975.
[27] N. Camarero, A. Trapero, A. Pérez-Jiménez, E. Macia, A. Gomila-Juaneda, A. Martin-Quiros, L. Nevola, A. Llobet, A. Llebaria, J. Hernando, *Chem. Sci.* **2020**, *11*, 8981–8988.
[28] C. Matera, A. M. J. Gomila, N. Camarero, M. Libergoli, C. Soler, P. Gorostiza, *J. Am. Chem. Soc.* **2018**, *140*, 15764–15773.
[29] F. A. Jerca, V. V. Jerca, R. Hoogenboom, *Nat Rev Chem* **2022**, *6*, 51–69.
[30] L. Chi, O. Sadovski, G. A. Woolley, *Bioconjugate Chem.* **2006**, *17*, 670–676.
[31] D. Bléger, J. Schwarz, A. M. Brouwer, S. Hecht, *J. Am. Chem. Soc.* **2012**, *134*, 20597–20600.
[32] R. Ger, *Br. Med. J.* **1964**, *2*, 295.
[33] D. M. Panczykowski, R. H. Jani, M. A. Hughes, R. F. Sekula Jr, *Neurosurgery* **2020**, *87*, 71–79.
[34] M. Bialer, *Epilepsia* **2012**, *53*, 26–33.
[35] A. A. Khan, N. Siddiqui, M. J. Akhtar, Z. Ali, M. S. Yar, *Arch Pharm (Weinheim)* **2016**, *349*, 277–292.
[36] K. Unverferth, J. Engel, N. Höfgen, A. Rostock, R. Günther, H.-J. Lankau, M. Menzer, A. Rolfs, J. Liebscher, B. Müller, *J. Med. Chem.* **1998**, *41*, 63–73.
[37] Q. Wu, J. Huang, X. Fan, K. Wang, X. Jin, G. Huang, J. Li, X. Pan, N. Yan, *Nat. Commun.* **2023**, *14*, 3224.
[38] M. Dong, A. Babalhavaeji, S. Samanta, A. A. Beharry, G. A. Woolley, *Acc. Chem. Res.* **2015**, *48*, 2662–2670.
[39] M. Walther, W. Kipke, R. Renken, A. Staubitz, *RSC Adv.* **2023**, *13*, 15805–15809.
[40] P. Lentes, E. Stadler, F. Röhricht, A. Brahms, J. Gröbner, F. D. Sönnichsen, G. Gescheidt, R. Herges, *J. Am. Chem. Soc.* **2019**, *141*, 13592–13600.
[41] E.-C. Elliott, J. L. Maggs, B. K. Park, P. M. O'Neill, A. V. Stachulski, *Org. Biomol. Chem.* **2013**, *11*, 8426–8434.

[42] S. Pittolo, X. Gómez-Santacana, K. Eckelt, X. Rovira, J. Dalton, C. Goudet, J.-P. Pin, A. Llobet, J. Giraldo, A. Llebaria, *Nat. Chem. Biol.* **2014**, *10*, 813–815.
[43] M. H. Berry, A. Holt, J. Levitz, J. Broichhagen, B. M. Gaub, M. Visel, C. Stanley, K. Aghi, Y. J. Kim, K. Cao, *Nat. Commun.* **2017**, *8*, 1862.
[44] M. Hammerich, C. Schütt, C. Stähler, P. Lentes, F. Röhricht, R. Höppner, R. Herges, *J. Am. Chem. Soc.* **2016**, *138*, 13111–13114.
[45] K. Rustler, G. Maleeva, A. Gomila-juaneda, P. Gorostiza, P. Bregestovski, **n.d**.
[46] D. A. Guggiana-Nilo, F. Engert, *Front Behav Neurosci* **2016**, *10*, 160.
[47] M. J. Y. Zimmermann, N. E. Nevala, T. Yoshimatsu, D. Osorio, D.-E. Nilsson, P. Berens, T. Baden, *Curr. Biol.* **2018**, *28*.
[48] C. Maximino, T. M. de Brito, A. W. da Silva Batista, A. M. Herculano, S. Morato, A. Gouveia Jr, *Behav. Brain Res.* **2010**, *214*, 157–171.
[49] E. V. Kysil, D. A. Meshalkina, E. E. Frick, D. J. Echevarria, D. B. Rosemberg, C. Maximino, M. G. Lima, M. S. Abreu, A. C. Giacomini, L. J. G. Barcellos, *Zebrafish* **2017**, *14*, 197–208.
[50] A. V. Kalueff, M. Gebhardt, A. M. Stewart, J. M. Cachat, M. Brimmer, J. S. Chawla, C. Craddock, E. J. Kyzar, A. Roth, S. Landsman, *Zebrafish* **2013**, *10*, 70–86.
[51] F. Emran, J. Rihel, J. E. Dowling, *J Vis Exp* **2010**.
[52] J. Staddon, R. Macphail, S. Padilla, *Nature Precedings* **2009**, *1*.
[53] T. S. Hahm, H. J. Ahn, S. Ryu, M. S. Gwak, S. J. Choi, J. K. Kim, J. M. Yu, *Br. J. Anaesth.* **2012**, *109*, 968–974.
[54] Y.-C. Yang, C.-S. Huang, C.-C. Kuo, *The Journal of the American Society of Anesthesiologists* **2010**, *113*, 160–174.
[55] I. Niespodziany, N. Leclère, C. Vandenplas, P. Foerch, C. Wolff, *J. Neurosci. Res.* **2013**, *91*, 436–443.
[56] L. Heintze, D. Schmidt, T. Rodat, L. Witt, J. Ewert, M. Kriegs, R. Herges, C. Peifer, *Int. J. Mol. Sci.* **2020**, *21*, 8961.
[57] M. Kammerer, B. Brawek, T. M. Freiman, R. Jackisch, T. J. Feuerstein, *Naunyn-Schmiedeberg's Arch. Pharmacol.* **2011**, *383*, 531–542.
[58] P. D. Bregestovski, G. V. Maleeva, *Neurosci. Behav. Physiol.* **2019**, *49*, 184–191.
[59] M. Schoenberger, A. Damijonaitis, Z. Zhang, D. Nagel, D. Trauner, *ACS Chem. Neurosci.* **2014**, *5*, 514–518.
[60] W. A. Velema, W. Szymanski, B. L. Feringa, *J. Am. Chem. Soc.* **2014**, *136*, 2178–2191.
[61] J. A. Frank, M.-J. Antonini, P.-H. Chiang, A. Canales, D. B. Konrad, I. C. Garwood, G. Rajic, F. Koehler, Y. Fink, P. Anikeeva, *ACS Chem. Neurosci.* **2020**, *11*, 3802–3813.
[62] J. H. Lee, S. Lee, D. Kim, K. J. Lee, *Adv. Drug Delivery Rev.* **2022**, *187*, 114399.
[63] R. Sortino, M. Cunquero, G. Castro-Olvera, R. Gelabert, M. Moreno, F. Riefolo, C. Matera, N. Fernàndez-Castillo, L. Agnetta, M. Decker, *Angew. Chem. Int. Ed.* **2023**, *62*, e202311181.
[64] M. Banghart, K. Borges, E. Isacoff, D. Trauner, R. H. Kramer, *Nat. Neurosci.* **2004**, *7*, 1381–1386.
[65] D. L. Fortin, M. R. Banghart, T. W. Dunn, K. Borges, D. A. Wagenaar, Q. Gaudry, M. H. Karakossian, T. S. Otis, W. B. Kristan, D. Trauner, *Nat. Methods* **2008**, *5*, 331–338.
[66] M. R. Banghart, A. Mourot, D. L. Fortin, J. Z. Yao, R. H. Kramer, D. Trauner, *Angew. Chem. Int. Ed.* **2009**, *48*, 9097–9101.
[67] A. Mourot, M. A. Kienzler, M. R. Banghart, T. Fehrentz, F. M. E. Huber, M. Stein, R. H. Kramer, D. Trauner, *ACS Chem. Neurosci.* **2011**, *2*, 536–543.
[68] V. A. Gutzeit, A. Acosta-Ruiz, H. Munguba, S. Häfner, A. Landra-Willm, B. Mathes, J. Mony, D. Yarotski, K. Börjesson, C. Liston, *Cell Chem. Biol.* **2021**, *28*, 1648–1663.
[69] A. Landra-Willm, A. Karapurkar, A. Duveau, A. A. Chassot, L. Esnault, G. Callejo, M. Bied, S. Häfner, F. Lesage, B. Wdziekonski, *Nat. Commun.* **2023**, *14*, 1160.
[70] M. Stein, S. J. Middendorp, V. Carta, E. Pejo, D. E. Raines, S. A. Forman, E. Sigel, D. Trauner, *Angew. Chem. Int. Ed.* **2012**, *51*, 10500–10504.
[71] J. Montnach, L. A. Blömer, L. Lopez, L. Filipis, H. Meudal, A. Lafoux, S. Nicolas, D. Chu, C. Caumes, R. Béroud, *Nat. Commun.* **2022**, *13*, 417.
[72] J. Montnach, H. Millet, A. Persello, H. Meudal, S. De Waard, P. Mesrica, B. Ribeiro, J. Richard, A. Hivonnait, A. Tessier, *Circ. Res.* **2023**, *133*, 535–538.
[73] A. V. Elleman, G. Devienne, C. D. Makinson, A. L. Haynes, J. R. Huguenard, J. Du Bois, *Nat. Commun.* **2021**, *12*, 4171.
[74] X. Rovira, A. Trapero, S. Pittolo, C. Zussy, A. Faucherre, C. Jopling, J. Giraldo, J.-P. Pin, P. Gorostiza, C. Goudet, *Cell Chem. Biol.* **2016**, *23*, 929–934.
[75] S. P. McClain, X. Ma, D. A. Johnson, C. A. Johnson, A. E. Layden, J. C. Yung, S. T. Lubejko, G. Livrizzi, X. J. He, J. Zhou, *Neuron* **2023**, *111*, 3926–3940.

Manuscript received: February 21, 2024
Accepted manuscript online: June 18, 2024
Version of record online: August 14, 2024